IEEE Access
Multidisciplinary ⋮ Rapid Review ⋮ Open Access Journal

Received 31 January 2023, accepted 25 February 2023, date of publication 7 March 2023, date of current version 25 April 2023.

Digital Object Identifier 10.1109/ACCESS.2023.3253203

RESEARCH ARTICLE

Finger Vein Recognition Based on Anatomical Features of Vein Patterns

ARYA KRISHNAN[1] **AND TONY THOMAS**[2]

[1]Indian Institute of Information Technology and Management-Kerala, (Research Center, Cochin University of Science and Technology), Trivandrum 695581, India

[2]School of Computer Science and Engineering, Kerala University of Digital Sciences, Innovation and Technology, Thiruvananthapuram, Kerala 695317, India

Corresponding author: Arya Krishnan (dr.aryakrishnan32@gmail.com)

This work was supported by the Center for Research and Innovation in Cyber Threat Resilience Project funded by Kerala State Planning Board under Grant CRICTR 2022-23.

ABSTRACT Finger vein recognition is a promising biometric authentication technique that depends on the unique features of vein patterns in the finger for recognition. The existing finger vein recognition methods are based on minutiae features or binary features such as LBP, LLBP, PBBM etc. or from the entire vein pattern. However, the minutiae-based features cannot accurately represent the structural or anatomical aspects of the vein pattern. These issues with the minutia feature led to increased false matches. Recognition based on binary features have limitations such as increased false matches, sensitivity to the translation and rotation, security and privacy issues etc. A feature representation based on the anatomy of vein patterns can be an alternative solution to improve the recognition performance. In the IJCB 2020 conference, we showed that every finger vein image contains one or more of a kind of 4 special vein patterns which we refereed as Fork, Eye, Bridge, and Arch (FEBA). In this paper, we further enlarge this set to 6 vein patterns ($F_1F_2EB_1B_2A$) by identifying two variations in the Fork and Bridge vein patterns. Based on 6 anatomical features of the possible 6 vein patterns in a vein image, we define a 6×6 feature matrix representation for finger vein images. Since this feature representation is based on the anatomical properties of the local vein patterns, it provides template security. Further we show that, the proposed feature representation is invariant to scaling, translation, and rotation changes. The experimental results using two open datasets and an in-house dataset show that the proposed method has a better recognition performance when compared to the existing approaches with an EER around 0.02% and an average recognition accuracy of 98%.

INDEX TERMS FEBA classification, F^2EB^2A, feature representation, finger vein biometrics, matching, vein anatomy.

I. INTRODUCTION

Recently, finger vein recognition has attracted considerable attention due to its contactless acquisition, intrinsic nature and high security. Finger vein recognition biometric trait is a significant biometric modality that is regarded as more secure, reliable, and emerging [1], [2]. Methods for finger vein recognition can be broadly classified into two categories depending on the type of the feature being used: image-based and vein pattern-based. The image-based methods [3], [4] extract features from both venous and non-venous regions of the vein image for recognition. The vein-pattern based approaches [5], [6], [7], on the other hand, leverage features from the vein structure for recognition. The vein pattern-based methods outperform image-based methods since they are based on the underlying vein pattern, which is the distinguishing characteristic of a vein image [7].

Some of the vein-pattern based methods [5], [6], [7], [8] initially extract the vein patterns from the image and then use the binary vein pattern as the feature. These approaches match the binary vein template with the input binary vein image using the matched pixel ratio [7]. However, direct vein template matching is prone to security and privacy threats. Hence, these methods require additional mechanisms to protect the

The associate editor coordinating the review of this manuscript and approving it for publication was Marina Gavrilova.

vein templates. Moreover, direct matching ignores the discriminating features of the vein pattern like the morphology of the vein structure, anatomy etc. Minutiae is a major feature descriptor used for finger vein images [9]. Methods based on the minutiae points, extract bifurcation and endpoints from the binary vein pattern and perform matching using distance measures [10]. However, the recognition accuracy of these methods are generally unsatisfactory since the minutiae points are very few in finger vein images. Furthermore, matching points are challenging due to the rotation, translation, and scale variations. There exists vein pattern-based methods that extract features like minutiae [9], SIFT [3], LBP [10] etc. from the vein structure and utilize these features for matching. Features like SIFT, has been extracted from vein patterns for recognition [3]. However, the performance of these methods can also get degraded under the effect of image variations. LBP [10], LLBP [4] use pixel intensity differences of each pixel in the vein image to generate the binary code for recognition. Since they are dependent on the pixel intensities of the entire vein image rather than the vein pattern specifically, variations caused by image intensity changes may have a negative impact on recognition performance. To effectively identify individuals, a feature based on the anatomy of the vein pattern can be used since the anatomical properties of the vein pattern can more robustly describe the features [11].

In the IJCB 2020 conference [12], we showed that every finger vein image contains one or more of a kind of 4 special vein patterns which we refereed as Fork, Eye, Bridge, and Arch (FEBA). Based on this observation we showed that there exists a fundamental anatomical classification for finger veins analogous to the Henry classification for fingerprints [11]. A CNN was designed to perform the classification task and an identification mechanism was proposed based on the classification. In this paper, we further enlarge the set of 4 vein patterns (FEBA) to 6 patterns ($F_1F_2EB_1B_2A$) by identifying two variations in the Fork (Up/Down Fork) and Bridge (Acute/Obtuse Bridge) vein patterns. We refer to the set of these 6 vein patterns as the F^2EB^2A patterns. Since the focus of this paper is on feature representation and matching we do not discuss about a classification scheme based on these patterns. Based on 6 anatomical features of the possible 6 vein patterns in a vein image, we define a 6 $\times$ 6 feature matrix representation for finger vein images. The anatomical features include the number of vein patterns, location, curvature, eccentricity, number of tributaries, and angle between the parent and branch veins. The 6 $\times$ 6 feature matrix is taken as the biometric template and is used for the recognition. To the best of our knowledge, this is the first work that utilizes the anatomical features of finger vein for recognition.

A. CONTRIBUTIONS

It is a known fact that if the original vein image is compromised, the finger vein biometric systems can be deceived [13]. Furthermore, recently it was demonstrated in [14] that it is possible to reconstruct the original image from a binary vein image. The proposed method is hard to spoof as the template generation is based on the anatomical features of local anatomical structures rather than the global binary vein pattern. Reconstructing the vein pattern from a template with feature values of local structures would be challenging. Besides, the proposed features are invariant to image scaling, translation, and rotation. The major contributions in this extension of [12] are summarized below.

1) The set of 4 fundamental vein patterns FEBA identified in [12] is enlarged to 6 patterns $F_1F_2EB_1B_2A$ by identifying two variations in the Fork (Up/Down Fork) and Bridge (Acute/Obtuse Bridge) vein patterns.
2) Based on the 6 anatomical features of the possible 6 vein patterns ($F_1F_2EB_1B_2A$) in a vein image, a 6 $\times$ 6 feature matrix representation for finger vein images is proposed. The anatomical features include the number of vein patterns, location, curvature, eccentricity, number of tributaries, and angle between the parent and branch veins. The 6 $\times$ 6 feature matrix is taken as the biometric template and is used for the recognition. The features are invariant to image translation, rotation and scaling.

Most of the existing feature representation approaches are designed based on the characteristics of the image rather than the vein pattern. These characteristics are less discriminative and can be influenced by image variations such as rotation, scaling, and translation. Hence, these features may not recognize the vein images accurately. In contrast to existing features for vein images, the proposed features are based on the anatomical classification of vein images. From the vein images, special patterns are identified, and anatomical features such as number, location, angle, curvature, and so on are retrieved. The properties obtained from these class patterns are fundamental to vein images, and hence they can effectively discriminate vein images. Hence, the proposed method can improve the recognition accuracy significantly which is proved in detail in the experimental section.

B. LIMITATIONS

Since the proposed method is based on the anatomy of vein patterns, the efficiency of the vein pattern pre-processing and extraction methods can have an impact on the proposed features. However, we have used the most commonly used state-of-the-art approaches for pre-processing [6] and vein pattern extraction [15]. Even though all of the vein images undergo refinement of the extracted vein patterns, the proposed recognition accuracy could be affected by the quality of the vein images. However, to further enhance the quality of the vein image, image restoration or enhancement methods like [16] can be used. The vein pattern extraction can be further improved by using vein extraction methods like [7].

II. RELATED WORKS

Finger vein recognition methods fall into two categories based on the features being used: image based and vein pattern based. Since the vein patterns are the distinguishing features of a vein image, features based on them were shown to perform better than approaches based on the whole images [6]. In this section, we discuss the state-of-the-art feature representations based on vein patterns extracted from vein images or vein images themselves.

In vein pattern-based methods [6], [7], the hidden patterns are extracted from the vein images initially. Then, the extracted vein patterns are stored as vein templates. Recognition is performed by directly matching the stored binary vein templates with the test vein templates. In methods such as [5], [6], and [7] matched pixel ratio is used to determine whether a test vein pattern belongs to a legitimate user or not. However, most of these vein template matching-based methods are sensitive to the variations in the vein image. Even though mechanisms like [17] had been proposed to deal with the variations in the vein image, they have a high computational overhead.

In minutiae-based methods [18], [19], and [9], discrete points are identified from the vein pattern for matching and recognition. In contrast to direct vein template matching, these methods match the characteristic points from the vein patterns to establish identity and the template size is relatively small for these methods. In most of the methods [9], matching is done by comparing the minutiae pairs using distance measures. However, the accuracy of minutiae-based methods are generally low since finding correspondence to the minutiae pair in vein images with variations is challenging. Another drawback of these methods is that feature descriptors based on minutiae points are insufficient for reliably recognizing individuals.

In [3], a method based on SIFT features was proposed for finger vein recognition. However, the SIFT key-points were not robust to variations due to scaling, translation and rotation in the vein images. A feature based on the structure of the vein was proposed in [20]. Here, the vein structures were considered as curve segments and the features of these curves were encoded as feature vectors for each pattern. A modified angular chain code was used to describe the curve segments extracted from the vein patterns. However, the size of the feature vector was high as it stores the angular code for curves traced from all the junction points and it may also get affected by the image variations.

In [19], a modified LPB based feature was proposed for better recognition of finger veins. LBP-based methods encode vein patterns into binary codes based on pixel intensity differences from the vein image. Rather than extracting vein patterns from the entire vein image, this method uses the whole vein image. The local areas in the vein images were classified using an SVM as having a small amount, a large amount, or a medium amount of vein pattern present. Then the LBP code was given a weight based on the local area category corresponding to the image patch. In [21] another approach based on LBP is proposed. However, these methods are sensitive to the translations and rotation of the finger.

A tri-branch structure-based recognition was proposed in [5]. However, this method contributes to improving the matching performance by utilizing the vein structure rather than utilizing the features from it. This approach uses the vein-pattern as the template and uses it for matching. Hence, a template protection mechanism is required to protect the vein templates to avoid data breaches.

An anatomical structural analysis-based finger vein recognition was proposed in [6]. The anatomical characteristics identified in [6] for refinement of the extracted vein pattern include continuity, solidness, directionality, and so on. However, the anatomical properties that have been considered are generic and apply to all vein patterns. These characteristics have not been employed as a feature but are used to address issues such as burrs, breaks, and gaps in the extracted vein network. The vein template is used as the feature in this work. Hence, a template protection mechanism is required to protect the vein templates to enhance the security of the system.

For the detection of finger veins, many deep feature learning methods such as [22] and [23] have been proposed recently. A CNN model is proposed in [24] that is trained using vein images for recognition based on the feature retrieved by the model. In [25] a deep representation model is designed to extract the vein patterns from the vein image. Deep learning-based methods learn different features based on the training images and the model that is being used. However, deep learning models require a large dataset to train the model accurately. Most of the method reduces the size of the original image which adversely affects the efficiency of the recognition. Furthermore, most of the deep learning methods train the models with the raw vein image. The model learns features from both venous and non-venous areas which can increase the chance of false matches [7].

The minutia-based methods [18] rely upon image coordinates for its location feature and the angle feature. The variations in scale, translation and rotation of the vein images have direct impact on the minutia features as they depend on coordinates of the image. Hence, the performance of minutia-based methods are low. SIFT based methods perform well on texture classification problems. However, the performance of SIFT features [3] are less discriminative for vein images as the image intensity variations adversely affects the recognition performance. Tri-branch based recognition [5] utilizes the tri-branch structure only for alignment of the vein structure. The method employs vein template matching for recognition. Here, user defined threshold learning and elastic matching is employed for recognition. However, the matching performance gets affected due to the rotation and translation variations. The performance of the angular-code based method [20] can degrade due to the effect of variations in the vein images. Since the CNN-FVR [24] utilized the vein images as such for training the model, deep model

may learn characteristics from the background pixels of the vein image that adversely affect the classification accuracy. Due to the training using incorrect labels generated by the baseline-methods employed for identifying the vein patterns, the performance of the Deep-FV [25] was degraded. Deep learning-based algorithms also necessitate a huge amount of data and a long computational time to train the model.

To address the various issues with the related works, we propose a feature representation technique that is based on the anatomical aspects of the vein pattern. Since it has already been shown that any vein pattern can be classified into four basic classes based on its anatomy, it will be possible to obtain the anatomical features for every vein pattern.

III. PROPOSED METHODOLOGY

This section describes the proposed feature representation technique based on the FEBA classification of the vein patterns [12] and the matching process. The recognition based on the proposed features is also discussed in detail. x Since the proposed approach leverages intrinsic features of the vein image, the vein patterns are extracted initially. In the proposed approach, the features of the 6 vein patterns $F_1F_2EB_1B_2A$ (Up/Down Fork, Eye, Acute/Obtuse Bridge, and Arch) present in the vein image are used for accurate recognition. The initial step is to locate and extract $F_1F_2EB_1B_2A$ patterns present in the vein image. Then, a 6×6 feature matrix is generated from the 6 class patterns. To authenticate a person, matrix matching is performed.

A. ANATOMY OF PALMAR FINGER VEINS

In [12], a classification scheme for finger veins was proposed based on the anatomical knowledge and visual characteristics of the vein structure in the palmar side (side of the finger where the fingerprints are present) of the finger. A set of 4 special vein patterns which we refereed as Fork, Eye, Bridge, and Arch (FEBA) was identified in finger vein images. Based on the existence of these vein patterns a classification scheme for finger vein images into 4 classes was proposed.

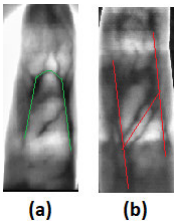

FIGURE 1. The special vein patterns identified from a vein image based on the vein types defined in [12]. (a) shows vein image having the vein type SVA and (b) shows vein image having the vein type SAV.

A study by Nystrom et al. [26] on the anatomy of palmar finger veins was used as the base for validating the observations and findings to establish the vein image classification. Superficial Venous Arches (SVA) and Superficial Axial Veins (SAV) as shown in 1 are the two main vein types that may be found in a finger. The SAV is a vein that runs parallel to the long axis of the finger. In a finger, there can be one or more SAVs that connect to one another through branches. SAVs are present in all vein images, and the number, position, branching, and other characteristics of these veins make each vein image unique. SVA is an arch-shaped vein that joins two SAVs and contains tributaries but no branches of its own. SVAs may or may not be present in all vein images. It can be observed from Fig.1(a) that the SVA has an arch shape and it connects two parallel veins. The parallel veins that run along the long axis of the finger as given in Fig.1(b) represents SAVs. Each class was defined based on the anatomical properties of the vein types (SAV and SVA) and the visual observations from the vein images.

The reference model of finger used for classification is shown in Fig.2.

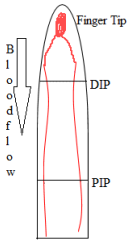

FIGURE 2. Reference model of finger.

B. F^2EB^2A: CLASSIFICATION OF FINGER VEIN PATTERNS

This section details about the FEBA vein patterns and the variations in the F and B patterns. We obtain a set of 6 different vein patterns $F_1F_2EB_1B_2A$ from the original set of 4 vein patterns F,E,B,A. We refer to this set of 6 vein patterns as F^2EB^2A patterns.

1) FORK PATTERNS: F_1, F_2

The Fork pattern is characterized by the presence of a "Y" like structure in the vein pattern and we call these structures as forks. This structure is formed by the sub-branches of the major veins. There exist several variations in this vein pattern. We identified two types of Fork patterns: Up Fork (F_1) and Down Fork (F_2), based on the visual observation that the Y patterns can occur as pointed upwards and downwards. An F_1 pattern is a Y like structure pointed in the upward direction as shown in Fig. 3(a). An F_1 pattern is a Y like structure pointed in the downward direction as shown in Fig. 3(b). It can be observed that the patterns belonging to these classes are mostly seen as forks.

2) EYE PATTERN

This pattern resembles the shape of a loop as shown in Fig.4. The pattern differs from the closed region generated by two lines connecting two SAVs. This pattern is formed by the merging of the branches that bend around and cross itself, as seen in Fig.4.

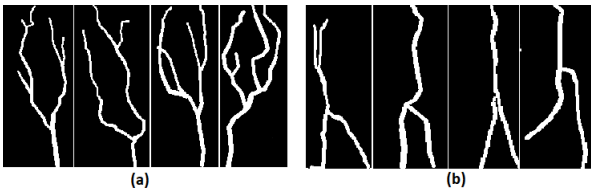

FIGURE 3. (a) Variations in the vein patterns of type F_1 (b) variations in the vein patterns of type F_2.

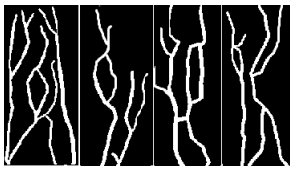

FIGURE 4. Variations in the Eye pattern.

3) BRIDGE PATTERNS: B_1, B_2

A Bridge (B_1, B_1) is bridge like vein pattern connecting two SAVs as shown in Fig. 5. The key requirement of the connection is that it should be a direct connection. The visual characteristic of this class is the presence of an ''H'' like pattern in the vein images. There exists variations in the Bridge class patterns. A combination of Down Fork and Up Fork (branch of a SAV that acts as a tributary to another SAV) are present in vein images that belong to this class.

The variations in this class is identified based on the angle the bridge makes with respect to the SAV from which it branches. A vein pattern is said to be Bridge B_1 if it forms a bridge making an acute angle with the parent vein as shown in Fig.5(a).

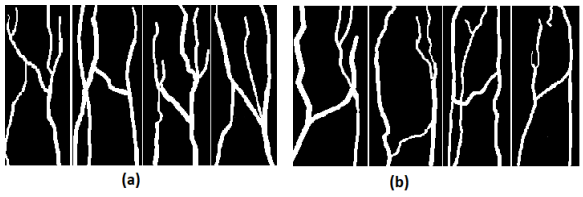

FIGURE 5. (a) Variations in the vein patterns of type B_1 (b) variations in the vein patterns of type B_1.

A vein pattern is said to be Bridge B_2, if it forms a bridge making an obtuse angle on the parent vein as shown in Fig. 5 (b).

The different types of branches are illustrated in Fig.6. It can be observed from Fig.6 that the branching vein always makes an acute angle with the parent vein and forms a Down Fork. The recipient vein and tributary together form an Up Fork.

4) ARCH PATTERN

A vein pattern is said to be an Arch if it has an arch like shape connecting two SAVs as shown in Fig. 7. This vein type has only tributaries, comparable to the SVA vein type.

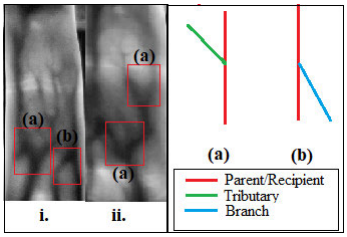

FIGURE 6. Vein branching based on palmar venous anatomy.

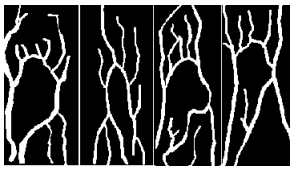

FIGURE 7. Variations in the Arch pattern.

It is always convex in shape and occurs between two SAVs. The arch generally has a few lines connecting it, forming a sunburst-like pattern. Variations were found in the arch pattern depending on the position and orientation of the arch. However, these variations are not enough to design subclasses based on them.

In this paper, we utilize the characteristics of the vein patterns to extract the features of the vein image. We describe these features in detail in Section III-D.

C. IDENTIFICATION AND EXTRACTION OF F^2EB^2A PATTERNS FROM BINARY VEIN IMAGE

A vein image contains at least one pattern or a combination of patterns, as detailed in Section IV. This section details the preliminary steps used to identify the F^2EB^2A vein patterns in a vein image. First the vein images have to be rotated in accordance with the anatomical reference model (Fig.2) for the finger. It is important to make sure that all the images are processed only in this direction since all the anatomical observations are drawn based on this reference model. The steps to identify all the possible Up Fork, Down Fork, Eye, Acute Bridge, Obtuse Bridge and Arch ($F_1F_2EB_1B_2A$) present in a vein image are given below. This involves locating Y shapes, loops and arches present in the image.

1) To identify the presence of 'Y' shapes, the bifurcation points in the binary vein image is utilized. The bifurcation points can be traced to find out the Y patterns. The located Y patterns are further characterized as upward Y or downward Y based on the vertex of a triangle fitted using the edges of the the Y structure. The y-coordinate of the top vertex of the triangle (end point of the parent vein) and the y-coordinate of the bifurcation point are compared to distinguish between downward Y and upward Y. For an upward Y the y-coordinate of the bifurcation point will be less than the y-coordinate of the top vertex of the triangle as shown in Fig.8(a) and (b). In the case of downward Y,

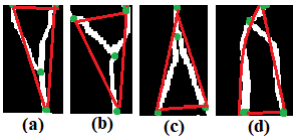

FIGURE 8. Samples of various Y types. (a) and (b) show sample image patch having an 'upward Y' (Up Fork). (c) and (d) show sample image patch having a 'downward Y' (Down Fork).

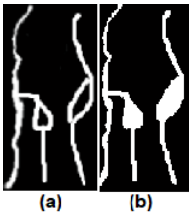

FIGURE 9. Sample vein image with Eye patterns. (a) shows a binary vein image with two Eye patterns and (b) shows the identified filled regions of holes present in the vein image.

the y-coordinate of the top vertex will be less than the bifurcation point as evident from Fig.8(c) and (d).

2) To check the presence of loops in the binary vein image, Euler number is used. Mathematically, Euler number, E of a binary image can be calculated as,

$$E = N - H, \tag{1}$$

where N is the number of connected components of the object in the binary image and H is the number of isolated regions in the background of the image. Depending on the value of E, we can detect whether the given vein pattern has loop or loops as shown in Fig.9(a) and (b). If $E = N$, then there exists no loop because, the number of holes will be zero in that case. If $E < N$ then, there exists at least one loop in the given image.

3) To locate arch in a vein image, circular Hough transform [27] is used. The circular Hough can locate semi-circle or arch-like structures in an image.

4) In a vein image, all the Y's occurring in the upward direction (without a downward Y following) are taken as Up Forks (F_1), all the Y's occurring in the downward direction (without an upward Y following) are taken as Down Forks (F_2), all the loops occurring are taken as Eyes (E), and the aches occurring are takes as Arches (A).

5) If the vein image contains combination of an upward Y and downward Y(an upward Y followed by a downward Y sharing a line), then this combination is taken an Acute Bridge (B_1). Similarly, if the vein image contains combination of downward Y and an upward Y(a downward Y followed by an upward Y sharing a line), then this combination is taken an Obtuse Bridge (B_2).

After identifying the locations of the F^2EB^2A patterns in the input binary image, we extract each of them using a bounding box. A circumscribed rectangle, or a bounding box, is the smallest rectangle that can be drawn around a set of points such that all the points are inside it [28].

The bounding box of a Fork pattern is defined based on the bifurcating point and the three end points of the structures as shown in Fig.10(a). From these four points, top-most, lowest, left-most and right-most points are identified by comparing their (x, y) coordinate values. The bounding boxes for Bridge and Arch patterns are defined based on the points of starting and ending of the connecting vein branch. The binary image is traced a fixed number of pixels (15 pixels) upwards and downwards from the starting point and ending point of the connecting vein branch to get the entire shape of the pattern. The endpoints of these traced lines along with the starting and ending points of the connecting vein branch are used to define the coordinates of the bounding boxes similar to Fork pattern. Fig.10 (c) and (d) show the bounding boxes of Bridge and Arch patterns respectively. The Eye patterns have holes and hence they are identified in the binary image using the Euler number. These holes can be extracted using binary image region measurement algorithms [29] that returns the locations of pixels in a specific region. Fig.10(b) shows the Eye patterns detected in the vein image.

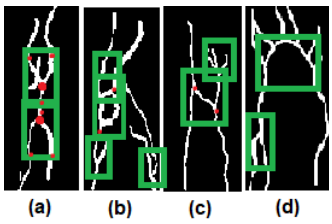

FIGURE 10. Bounding boxes on various patterns. (a) Fork (F_1 and F_2) patterns, (b) Fork (F_1) and Eye pattern, (c) Bridge (B_1) and a Fork (F_1) patterns and (d) a Fork (F_2) and an Arch pattern.

D. FEATURE MATRIX AND FEATURE EXTRACTION

Features specific to F^2EB^2A patterns in a vein image are extracted and are represented as a feature matrix of the size 6×6. The rows of the feature matrix correspond to the 6 features: c (number of F^2EB^2A patterns), p (anatomical position of various patterns), κ (curvature of various patterns), θ (angle between bifurcations in a pattern), e (eccentricity of the ellipse fitting the Eye pattern), a (number of tributaries to the Arch pattern). The columns correspond to the 6 patterns F_1, F_2, E, B_1, B_2 and A. The $(i, j)^{\text{th}}$ element of the matrix corresponds to the i^{th} feature of the j^{th} pattern present in the vein image. The $(i, j)^{\text{th}}$ element of the matrix will be zero if the j^{th} pattern is not present in the image or the i^{th} feature is not applicable to the j^{th} pattern. Hence, the feature matrix has the form as shown in Fig 11.

The details of various feature and the feature extraction are described below.

Feature c: The feature c denotes the number of F^2EB^2A patterns present in the image.

Feature p: The feature p denotes the anatomical position of the F^2EB^2A patterns present in the vein image. Here,

	F_1	F_2	E	B_1	B_2	A
Count(c)						
Position(p)						
Curvature(κ)						
Angle(θ)			0			0
Eccentricity(e)	0	0		0	0	0
Tributaries(a)	0	0	0	0	0	

FIGURE 11. The feature matrix with the 6 features as rows and the 6 patterns as columns.

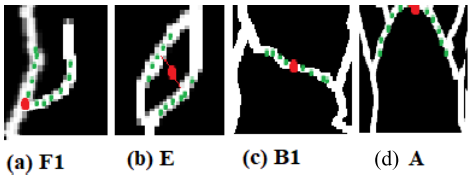

FIGURE 12. Curvature points of various class patterns. (a) curvature points of Fork (F_1) pattern, (b) curvature of an Eye pattern, (c) curvature of Bridge (B_1) pattern and (d) the curvature of an Arch pattern.

we determine the position of the vein structures based on the reference model given in Fig.2. The feature value is assigned based on the centriod of the whole vein pattern and the top most point of the particular pattern. If the top-most point of a pattern is below and far from the centriod, then the value -1 is assigned to p. If the top-most point of the vein pattern is near and close to the centriod, then the value 0 is assigned to p. If the top-most point of the class pattern is above and far from the centriod, then the value 1 is assigned to p.

Feature κ: The curvature feature is common to all the patterns. The curvature of 20 or sufficiently enough edge points are estimated as given in [30]. These edge points are selected based on bifurcation points or midpoints of the patterns as a reference point. For Fork patterns (F_1 and F_2), we utilize equally spaced 10 points on both sides of the bifurcating point for curvature estimation. In the case of Eye patterns, the mid points on both sides of the loop-structure are found using a line drawn from the center of the structure. Then, 10 points on both sides are selected to compute the curvature. For Bridge patterns (B_1 and B_2) and Arch patterns, the midpoint is found based on the end points of the bridging line or the arch. Then, 10 points each on left and right of the midpoint are taken.

Feature θ: The feature θ denotes the angle between two branches in a vein pattern. This feature is defined only for the Fork and Bridge patterns. For Fork (F_1 and F_2) pattern and Bridge pattern (B_1 and B_2), the angle θ is defined as the angle formed between the branches from the bifurcating points. Fig.13 shows the angle computation in Bridge and Fork patterns.

Feature e: This is a feature specific to the Eye pattern and it is based on the observation that the pattern Eye has an elliptic shape. Thus, an ellipse can be fitted on the eye pattern and the eccentricity of this ellipse is taken as the feature e.

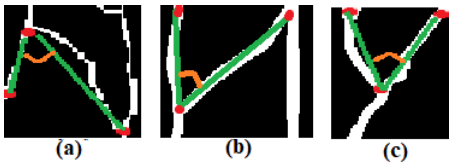

FIGURE 13. The branching angles of Bridge and Fork patterns.

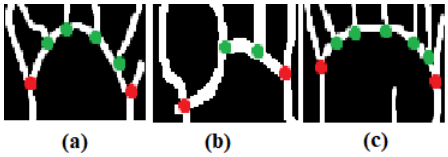

FIGURE 14. Arch patterns with varying number of normal lines.

Feature a: The Arch pattern appears to be a curved pattern with some lines normal to it (like a sun-burst) [12]. The number of such normals is taken as the feature a.

The number of bifurcating points within the Arch pattern are used to find the number of normals. Fig. 14 shows different Arch patterns with varying number of lines normal to it. Fig.14 (a) has $a = 4$, 14 (b) has $a = 2$ and 14 (c) has $a = 5$ as indicated by green color points in the image. The red color points indicate the start and end of the Arch connection.

It can be observed from that the feature matrix is it is created using the 6 features c, p, κ, θ, e and a and the 6 F^2EB^2A patterns. The features c, p and κ are defined for all the 6 patterns. The feature θ is defined for all patterns except Eye and Arch patterns. Hence, the feature value of θ for Eye and Arch patterns are 0. Similarly the feature e is defined only for the pattern Eye and a is defined only for the pattern Arch. Hence, the rest of the classes have 0 value corresponding to the features e and a. Each element in the feature matrix can be either a single value or a vector (when multiple patterns of same type occur).

If multiple patterns of the same type are present in a vein image, an order needs to be defined for the arrangement of their feature values at a position in the feature matrix. While scanning the whole vein image from left to right and top to bottom, the order in which a particular type of class pattern occurs is taken as the order of their feature values in the feature vector occurring at any row and column of the feature matrix.

E. MATCHING

The matching is performed by comparing the feature matrices of the registered vein image and the query vein image using matrix subtraction.

Let Q and T be the feature matrices corresponding to the query image and the registered vein image and $D = Q - T$ denotes the difference matrix. Each value in the difference matrix will be compared with a threshold value. Only one threshold will be needed for each feature (row of the difference matrix) as the differences among the features of various

TABLE 1. Distribution of vein images having one or more patterns.

Databases	Total Images	No. of images with atleast 1 pattern	No. of images combination of 2	No. of images combination of 3	No. of images combination of 4
HKPU	3132	2190	2100	82	8
SDUMLA	636	450	269	172	9
In-House	600	550	372	167	11

patterns are comparable. Thresholds ($t_1, t_2, t_3, t_4, t_5, t_6$) specific to the six feature (rows) are estimated based on the experimental evaluations. Each element in the difference matrix will be compared with the threshold corresponding to the row of that element. If all the elements in the difference matrix are below the thresholds then, it will be considered as a genuine match.

IV. RESULTS AND DISCUSSION

This section includes the description of datasets used, experimental results obtained and the comparison of performance with existing approaches.

Here, we have evaluated our approach based on two publicly available datasets (HKPU, SDUMLA) and our inhouse dataset. The HKPU [31] dataset contains finger vein images of 156 subjects with 6 images per subject taken in the two sessions. All the images are in BMP format and has a resolution of 513 × 256. The SDUMLA [32] has 636 unique vein images with 6 images per subject captured in one session. The images are in BMP format with a resolution of 320 × 240. The in-house dataset includes data captured from 100 subjects with 5 images per subject taken in one session. The images are in BMP format and with a resolution of 320 × 240. The distribution of vein images in the databases having various patterns (either as combinations of F^2EB^2A or atleast one of the four patterns) is given in Table 1. From the table, it can be noticed that in all the databases, almost all the vein images have atleast one of the special pattern present in them. We can also notice that the combinations of two patterns are more frequent than the combination of three and four.

A. IMPLEMENTATION DETAILS

The raw finger vein images were pre-processed [12] to remove noise and improve the quality of the image. In order to normalize the resolutions of the images from different databases, images were resized to 350 × 350 in the preprocessing stage. There was no significant loss of information in the vein pattern images due to the resizing process as it was performed after pattern extraction. The customary maximum curvature method was used for vein pattern extraction [15]. Post processing of the vein patterns was performed based on the anatomical structure analysis detailed in [6]. Some of the binary vein images given in this paper (for illustration purpose only) is taken from the ground truth images provided by Jalilian et al. [33].

B. PERFORMANCE EVALUATION

Experiments were carried out to evaluate the recognition performance of the proposed method. For evaluation, first three images of each subject were considered as registered templates and the rest of the images of each subject were used as the test templates.

The Equal Error Rate (EER), Zero False Match Rate (ZFMR), False Match Rate (FMR1000) metrics and Rank-1 recognition accuracy were used to evaluate the recognition performance of the proposed method and that of existing methods. The verification accuracy is higher when the EER, ZFMR, and FMR1000 values are low. We followed the biometrics test protocol of the fingerprint verification protocol FVC2004 [34] for calculating these metrics. The Rank 1 recognition accuracy is computed in the identification mode and the EER, ZFMR and FMR1000 are calculated in the verification mode.

Table 2 shows the recognition performance of the proposed method and the existing methods such as Minutia [18], SIFT [3], Angular-code [20], tri-branch [5], CNN-FVR [24] and Deep-FV [25] based on HKPU, SDUMLA and the inhouse datasets. The ROC curves of the existing methods like Angular code, Tribranch, Minutia, Deep Representation, CNN-FVR and the proposed method based on the datasets such as HKPU, SDUMLA and the inhouse are shown in Fig. 15, Fig. 16 and Fig. 17 respectively. It is evident from the ROCs that the proposed method outperforms the state-of-the-art methods.

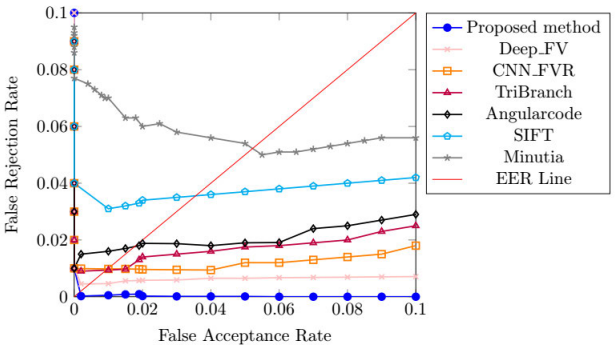

FIGURE 15. ROC of the matching performances using HKPU dataset.

C. DISCUSSION: PERFORMANCE EVALUATION

It can be observed from Tables 2 that the proposed method outperforms the existing methods in terms of all the metrics. The minutia-based methods [18] reply upon image coordinates for its location feature and the angle feature. SIFT based methods performs well on texture classification problems. However, the performance of SIFT features [3] are less discriminative for vein images as the image intensity variations adversely affects the recognition performance.

TABLE 2. Performance comparison using HKPU, SDUMLA and in-house datasets.

HKPU				
Method	EER (%)	ZFMR (%)	FMR1000 (%)	Recognition Accuracy (%)
Minutia [18]	5.35	8.16	8.51	60.13
SIFT [3]	3.11	6.22	6.01	76.33
Angular-code [20]	1.02	4.23	4.02	83.43
Tri-branch [5]	0.52	3.41	4.33	86.14
CNN-FVR [24]	0.5	2.23	2.01	90.22
Deep-FV [25]	0.08	1.21	1.35	93.12
Proposed Method	0.02	0.56	0.83	98.23
SDUMLA				
Method	EER (%)	ZFMR (%)	FMR1000 (%)	Recognition Accuracy (%)
Minutia [18]	8.33	8.12	9.11	59.55
SIFT [3]	7.12	6.22	7.27	75.33
Angular-code [20]	2.42	5.36	5.12	81.26
Tri-branch [5]	1.32	3.47	4.13	85.16
CNN-FVR [24]	0.67	3.03	2.31	90
Deep-FV [25]	0.07	1.02	1.23	94.32
Proposed Method	0.03	0.46	0.73	97.28
IN-HOUSE				
Method	EER (%)	ZFMR (%)	FMR1000 (%)	Recognition Accuracy (%)
Minutia [18]	7.17	8.06	8.41	60.21
SIFT [3]	6.01	6.08	6.51	76.23
Angular-code [20]	5.46	4.23	5.15	81.51
Tri-branch [5]	1.42	4.01	4.26	85.05
CNN-FVR [24]	0.71	2.01	2.05	91.3
Deep-FV [25]	0.09	1.31	1.25	93
Proposed Method	0.02	0.46	0.73	98.26

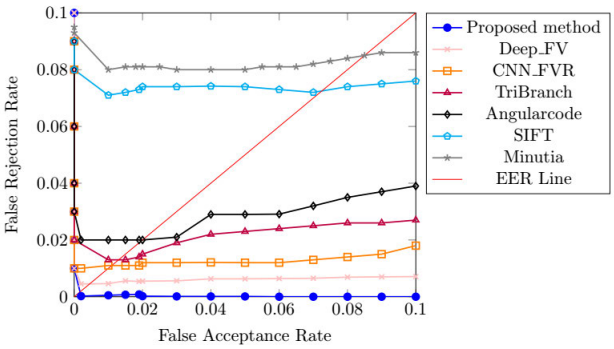

FIGURE 16. ROC of the matching performance using SDUMLA dataset.

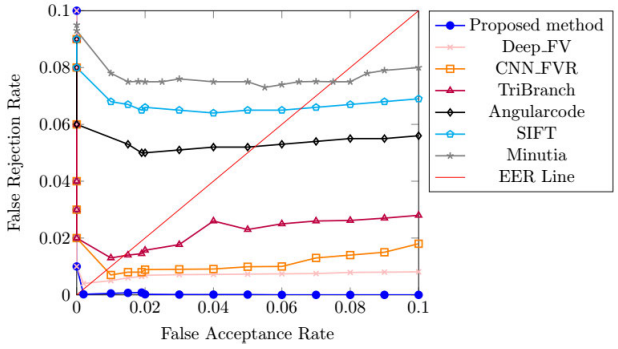

FIGURE 17. ROC of the matching performance using in-house dataset.

Tri-branch based recognition [6] utilizes the tri-branch structure only for alignment of the vein structure. The method employs vein template matching for recognition. Here, user defined threshold learning and elastic matching is employed for recognition. However, the matching performance gets affected due to the rotation, translation variations. The performance of Angular-code based method [20] also gets degraded due to the effect of variations in the vein images. The performance of the deep learning models [24], [25] are better than other approaches. However, the performance is low when compared to the proposed method mainly due to the fact that these based are trained based on raw vein images. The proposed method achieves better accuracy mainly due to the robustness in terms of image rotations, translation and scaling. This is due to the fact that the proposed method utilizes the anatomical features of local structures extracted from the vein image. In addition, the anatomical structures are more discriminative features of the vein patterns. Hence, a method based on such structures can improve the overall accuracy of a finger vein recognition system.

D. ROBUSTNESS EVALUATION

We evaluate the robustness of the proposed method based on variations that can influence the overall recognition performance of the system. Here, we analyse the performance under scaling, rotation and translation variations using the set of vein images from the in-house dataset. Here, the 'drop in performance' refers to the difference in performance (both EER and accuracy) without scaling or rotation or translation with that of maximum amount of scaling or translation or rotation.

The misplacement of finger while scanning the vein image can affect the recognition performance [35]. To evaluate the

TABLE 3. Performance comparison after rotating the images.

	±0		±10		±20		±30		Drop in performance	
Methods	EER	Accuracy (%)	EER	Accuracy (%)	EER	Accuracy(%)	EER	Accuracy(%)	EER	Accuracy(%)
Minutia [18]	7.17	60.21	15.04	56.3	20.05	50	30.03	39.23	22.86	21
SIFT [3]	6.01	76.23	7.31	72.46	8.24	70.12	8.05	70.03	2.04	6.2
Angular-code [20]	5.46	81.51	6.01	79.19	7.22	72.06	8.12	70.02	2.66	11.49
Tri-branch [5]	1.42	85.05	3.03	79.02	5.66	71.12	6.16	69.06	4.74	15.99
CNN-FVR [24]	0.71	91.3	1.32	85.5	2.02	84.23	4.5	80.3	3.79	11
Deep-FV [25]	0.09	93	0.86	87.32	1.10	86.34	1.35	85.15	1.26	7.85
Proposed Method	0.02	98.26	0.03	98.04	0.05	97.14	0.06	96.7	0.04	1.56

TABLE 4. Performance comparison after scaling down the images.

	without scaling		20		30		40		Drop in performance	
Methods	EER	Accuracy (%)	EER	Accuracy (%)	EER	Accuracy(%)	EER	Accuracy(%)	EER	Accuracy(%)
Minutia [18]	7.17	60.21	16.1	55	20.31	49.8	30.17	40	23	20
SIFT [3]	6.01	76.23	7	74.33	7.61	71.12	8.14	70.04	2.13	6.19
Angular-code [20]	5.46	81.51	7.01	71.1	7.37	70.06	8.19	70	2.73	11.51
Tri-branch [5]	1.42	85.05	2.03	83	3.12	80	6.16	6	4.74	17.69
CNN-FVR [24]	0.71	91.3	1.11	88.3	2.04	85.3	2.5	83.21	1.79	8.09
Deep-FV [25]	0.09	93	0.7	89.30	1.13	86.28	1.24	87.15	1.15	5.85
Proposed Method	0.02	98.26	0.04	98.02	0.05	97.02	0.06	96.32	0.04	1.94

TABLE 5. Performance comparison with translated images.

	without translation		20		30		40		Drop in performance	
Methods	EER	Accuracy (%)	EER	Accuracy (%)	EER	Accuracy(%)	EER	Accuracy(%)	EER	Accuracy(%)
Minutia [18]	7.17	60.21	20.01	50.12	22.45	43.01	24.03	40.13	16.86	20.08
SIFT [3]	6.01	76.23	6.31	74.46	7.3	70.17	7.21	70.05	1.2	6.11
Angular-code [20]	5.46	81.51	6.01	74	7.20	72	8.01	70.12	2.55	11.39
Tri-branch [5]	1.42	85.05	2.32	82.02	3.25	75.5	6.03	68.02	4.61	17.03
CNN-FVR [24]	0.71	91.3	0.82	91.1	0.85	91	1.12	90	0.41	1.3
Deep-FV [25]	0.09	93	0.74	92.5	1.13	92	1.24	91.4	1.15	1.6
Proposed Method	0.02	98.26	0.03	98.03	0.04	98.02	0.05	97.11	0.03	1.15

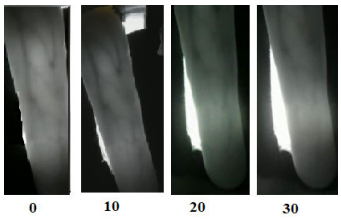

FIGURE 18. Sample vein images without rotation and with a rotation of +10, +20 and +30 degrees.

rotation invariance, we have considered the rotation of finger along the long axis of the finger.

We have obtained 50 vein images with rotation (only up to ±30 degree) to evaluate the robustness of the proposed method against longitudinal rotations of the finger. Fig.18 shows sample images with no rotation and with rotations of +10, +20 and +30 degrees respectively. We have compared the performance of the proposed and the existing approaches such as minutia [18], SIFT [3], tri-branch [5], angular-code [20], CNN-FVR [24] and Deep-FV [25]. The results of performance evaluation based on EER and recognition accuracy are shown in Table 3.

E. DISCUSSION: ROBUST EVALUATION

It can be observed from Table 3 that the EER and the recognition accuracy of the proposed method are not much affected by rotation. Although the SIFT features are invariant to affine transforms, for finger vein images SIFT features are less discriminative. This is due to the fact that SIFT features are extracted based on the vein images and the key points depend on image changes. Minutia based [18] and tri-branch based recognition [5] are less robust to rotation changes as they are defined based on pixel coordinates. The angular-code method [20] also gets affected by the rotation changes as the code is not normalized to provide rotation invariance. The performance of the deep learning models [24] and [25] are better when compared to other methods. However, when tested with an unseen dataset with rotational variations the recognition performances were found to be low. This is may be due to the fact that the features contained unseen variations compared to the training images.

We have scaled down 50 vein images from the in-house dataset by 25%, 35% and 45% of their original sizes and evaluated the performance of the proposed method and the existing methods. The performance results are shown in Table 4. It can be noticed that the performance of the proposed method is not much affected by scaling. The performance of SIFT [3] is affected as they extract features from the degraded gray-scale image. The performance of minutiae based methods, tri-branch and angular-code are low due to the fact that the matchings are done based on image coordinates. The performance of the deep learning models [24] and [25]

are also affected. This may be due to the fact that the features contained unseen variations compared to the training images.

Translation of vein images may occur when the user shifts the fingers (finger moves horizontally) while imaging. We have translated a set of 50 vein images by 20, 30 and 40 pixel positions along the x-direction. The performance of the proposed method and the existing methods are compared based on the EER. The Table 5 shows the EER and accuracy of the proposed method and the existing methods without translation and with the translations. It can be noticed that the performance of the proposed method is not much affected by translation. The performance of minutia and tri-branch methods are low as they depend on the image coordinates to define the features. The SIFT based method [3] and angular-codes [20] perform better than these methods. The performance of the deep learning models [24] and [25] were not much affected. However, the proposed approach outperforms significantly among all these methods.

V. CONCLUSION

In this paper, we proposed a novel feature representation and recognition method based on the anatomical classification of finger vein images. In the proposed approach, the classification based anatomical structures identified from the vein images are utilized for efficient recognition. We showed through extensive experiments that the proposed features are invariant to translation rotation and scaling and significantly reduces the recognition error rate compared to the existing vein based methods. The major future research directions are adding more number of sub-patterns to the fundamental F^2EB^2A patterns and improving the feature representation by incorporating more pattern based features.

REFERENCES

[1] K. Shaheed, A. Mao, I. Qureshi, M. Kumar, S. Hussain, and X. Zhang, "Recent advancements in finger vein recognition technology: Methodology, challenges and opportunities," *Inf. Fusion*, vol. 79, pp. 84–109, Mar. 2022.

[2] K. Shaheed, A. Mao, I. Qureshi, M. Kumar, Q. Abbas, I. Ullah, and X. Zhang, "A systematic review on physiological-based biometric recognition systems: Current and future trends," *Arch. Comput. Methods Eng.*, vol. 28, pp. 4917–4960, Feb. 2021.

[3] J. Peng, N. Wang, A. A. A. El-Latif, Q. Li, and X. Niu, "Finger-vein verification using Gabor filter and SIFT feature matching," in *Proc. 8th Int. Conf. Intell. Inf. Hiding Multimedia Signal Process.*, Jul. 2012, pp. 45–48.

[4] B. A. Rosdi, W. S. Chai, and S. A. Suandi, "Finger vein recognition using local line binary pattern," *Sensors*, vol. 11, no. 12, pp. 11357–11371, 2011.

[5] L. Yang, G. Yang, X. Xi, X. Meng, C. Zhang, and Y. Yin, "Tri-branch vein structure assisted finger vein recognition," *IEEE Access*, vol. 5, pp. 21020–21028, 2017.

[6] L. Yang, G. Yang, Y. Yin, and X. Xi, "Finger vein recognition with anatomy structure analysis," *IEEE Trans. Circuits Syst. Video Technol.*, vol. 28, no. 8, pp. 1892–1905, Aug. 2018.

[7] A. Krishnan, T. Thomas, and D. Mishra, "Finger vein pulsation-based biometric recognition," *IEEE Trans. Inf. Forensics Security*, vol. 16, pp. 5034–5044, 2021.

[8] G. R. Nayar, T. Thomas, and S. Emmanuel, "Graph based secure cancelable palm vein biometrics," *J. Inf. Secur. Appl.*, vol. 62, Nov. 2021, Art. no. 102991.

[9] C. B. Yu, H. F. Qin, and Y. Z. Cui, "Finger-vein image recognition combining modified Hausdorff distance with minutiae feature matching," *Interdiscipl. Sci. Comput. Life Sci.*, vol. 1, no. 4, pp. 280–289, 2009.

[10] K.-Q. Wang, A. S. Khisa, X.-Q. Wu, and Q.-S. Zhao, "Finger vein recognition using LBP variance with global matching," in *Proc. Int. Conf. Wavelet Anal. Pattern Recognit.*, Jul. 2012, pp. 196–201.

[11] H. Faulds and W. J. Herschel, *Dactylography Origin Finger-Printing*. Cambridge, U.K.: Cambridge Univ. Press, 2015.

[12] A. Krishnan, G. R. Nayar, T. Thomas, and N. A. Nystrom, "FEBA—An anatomy based finger vein classification," in *Proc. IEEE Int. Joint Conf. Biometrics (IJCB)*, Oct. 2020, pp. 1–9.

[13] A. Krishnan, T. Thomas, G. R. Nayar, and S. S. Mohan, "Liveness detection in finger vein imaging device using plethysmographic signals," in *Proc. Int. Conf. Intell. Hum. Comput. Interact.* Cham, Switzerland: Springer, 2018, pp. 251–260.

[14] C. Kauba, S. Kirchgasser, V. Mirjalili, A. Uhl, and A. Ross, "Inverse biometrics: Reconstructing grayscale finger vein images from binary features," in *Proc. IEEE Int. Joint Conf. Biometrics (IJCB)*, Oct. 2020, pp. 1–10.

[15] N. Miura, A. Nagasaka, and T. Miyatake, "Extraction of finger-vein patterns using maximum curvature points in image profiles," *IEICE Trans. Inf. Syst.*, vol. 90, no. 8, pp. 1185–1194, 2007.

[16] J. Yang and Y. Shi, "Towards finger-vein image restoration and enhancement for finger-vein recognition," *Inf. Sci.*, vol. 268, pp. 33–52, Jun. 2014.

[17] S. Pang, Y. Yin, G. Yang, and Y. Li, "Rotation invariant finger vein recognition," in *Chin. Conf. Biometric Recognit.* Cham, Switzerland: Springer, 2012, pp. 151–156.

[18] F. Liu, G. Yang, Y. Yin, and S. Wang, "Singular value decomposition based minutiae matching method for finger vein recognition," *Neurocomputing*, vol. 145, pp. 75–89, Dec. 2014.

[19] E. C. Lee, H. C. Lee, and K. R. Park, "Finger vein recognition using minutia-based alignment and local binary pattern-based feature extraction," *Int. J. Imag. Syst. Technol.*, vol. 19, no. 3, pp. 179–186, 2009.

[20] D. Cao, J. Yang, Y. Shi, and C. Xu, "Structure feature extraction for finger-vein recognition," in *Proc. 2nd IAPR Asian Conf. Pattern Recognit.*, Nov. 2013, pp. 567–571.

[21] Z. Zhang and M. Wang, "Multi-feature fusion partitioned local binary pattern method for finger vein recognition," *Signal, Image Video Process.*, vol. 16, no. 4, pp. 1091–1099, Jun. 2022.

[22] W. Liu, H. Lu, Y. Wang, Y. Li, Z. Qu, and Y. Li, "MMRAN: A novel model for finger vein recognition based on a residual attention mechanism," *Appl. Intell.*, vol. 53, no. 3, pp. 3273–3290, Feb. 2023.

[23] K. Shaheed, A. Mao, I. Qureshi, M. Kumar, S. Hussain, I. Ullah, and X. Zhang, "DS-CNN: A pre-trained xception model based on depth-wise separable convolutional neural network for finger vein recognition," *Expert Syst. Appl.*, vol. 191, Apr. 2022, Art. no. 116288.

[24] R. Das, E. Piciucco, E. Maiorana, and P. Campisi, "Convolutional neural network for finger-vein-based biometric identification," *IEEE Trans. Inf. Forensics Security*, vol. 14, no. 2, pp. 360–373, Feb. 2019.

[25] H. Qin and M. A. El-Yacoubi, "Deep representation-based feature extraction and recovering for finger-vein verification," *IEEE Trans. Inf. Forensics Security*, vol. 12, no. 8, pp. 1816–1829, Aug. 2017.

[26] Å. Nyström, G. V. Drasek-Ascher, J. Fridén, and G. D. Lister, "The palmar digital venous anatomy," *Scandin. J. Plastic Reconstructive Surg. Hand Surg.*, vol. 24, no. 2, pp. 113–119, Jan. 1990.

[27] P. Kierkegaard, "A method for detection of circular arcs based on the Hough transform," *Mach. Vis. Appl.*, vol. 5, no. 4, pp. 249–263, Sep. 1992.

[28] Y. Doytsher, "Defining a minimum area rectangle circumscribing given information," *Cartographic J.*, vol. 25, no. 2, pp. 97–103, Dec. 1988.

[29] P. K. Bhaskar and S.-P. Yong, "Image processing based vehicle detection and tracking method," in *Proc. Int. Conf. Comput. Inf. Sci. (ICCOINS)*, Jun. 2014, pp. 1–5.

[30] S. Al-Maadeed, A. Hassaine, A. Bouridane, and M. A. Tahir, "Novel geometric features for off-line writer identification," *Pattern Anal. Appl.*, vol. 19, no. 3, pp. 699–708, Aug. 2016.

[31] Y. Lu, S. J. Xie, S. Yoon, Z. Wang, and D. S. Park, "An available database for the research of finger vein recognition," in *Proc. 6th Int. Congr. Image Signal Process. (CISP)*, vol. 1, Dec. 2013, pp. 410–415.

[32] Y. Yin, L. Liu, and X. Sun, "SDUMLA-HMT: A multimodal biometric database," in *Proc. Chin. Conf. Biometric Recognit.* Cham, Switzerland: Springer, 2011, pp. 260–268.

[33] E. Jalilian and A. Uhl, "Enhanced segmentation-CNN based finger-vein recognition by joint training with automatically generated and manual labels," in *Proc. IEEE 5th Int. Conf. Identity, Secur., Behav. Anal. (ISBA)*, Jan. 2019, pp. 1–8.
[34] D. Maio, D. Maltoni, R. Cappelli, J. L. Wayman, and A. K. Jain, "FVC2004: Third fingerprint verification competition," in *Proc. Int. Conf. Biometric Authentication*. Cham, Switzerland: Springer, 2004, pp. 1–7.
[35] B. Prommegger, C. Kauba, M. Linortner, and A. Uhl, "Longitudinal finger rotation—Deformation detection and correction," *IEEE Trans. Biometrics, Behav., Identity Sci.*, vol. 1, no. 2, pp. 123–138, Apr. 2019.

ARYA KRISHNAN received the bachelor's and master's degrees in computer science from Amrita University, Kerala, India, in 2011 and 2013, respectively, and the M.Phil. degree in computer science from the Cochin University of Science and Technology (CUSAT), Kerala, in 2014, where she is currently pursuing the Ph.D. degree with the Indian Institute of Information Technology and Management-Kerala, Research Center. Her current research interests include biometric recognition, mainly focusing on finger vein biometrics, security, and image processing.

TONY THOMAS received the master's and Ph.D. degrees from IIT Kanpur. After completing his Ph.D. degree, he carried out his postdoctoral research with the Korea Advanced Institute of Science and Technology. After that, he joined as a Researcher with the General Motors Research Laboratory, Bengaluru, India. Later, he moved to the School of Computer Engineering, Nanyang Technological University, Singapore, as a Research Fellow. In 2011, he joined as an Assistant Professor with the Indian Institute of Information Technology and Management-Kerala (IIITM-K). He is currently an Associate Professor with the School of Computer Science and Engineering, Kerala University of Digital Sciences, Innovation and Technology, India (formerly IIITM-K). He is an Associate Editor of IEEE ACCESS and a reviewer of several journals. His current research interests include malware analysis, biometrics, cryptography, and machine learning applications in cyber security.